2022 IEEE 5th International Conference on Soft Robotics (RoboSoft)
April 4-8, 2022, Edinburgh, UK

A systematically derived design for a modular pneumatic soft bending actuator*

Frederik Lamping, Daniel Müller and Kristin M. de Payrebrune[1]

***Abstract*— In the field of pneumatic soft robots, arranging three air chambers in parallel is a common technique in order to build a bending actuator. Although these three chamber actuators are often used, many designs are based on trial and error, rather than on systematic investigation. In this study, we present a novel modular three chamber bending actuator. We derive beneficial design parameters from a systematic investigation that targets not only bending performance but also ease of fabrication and modeling. Due to its modularity, the bending actuator can be used as a "construction kit", i.e. a customized actuator can be build by combination of basic components. Furthermore, individual components of the actuator can be reused in another configuration, if desired. The characteristics of the actuator are identified experimentally. Its maximum bending and stretching is satisfying, but lower than that of the well-known "STIFF-FLOP" due to the reinforcement that was chosen to reduce the manufacturing effort.**

I. Introduction

The soft robotic community is growing and with it the number of proposed designs [1], [2]. Even when reducing the focus on pneumatic soft robots, many ideas on how to achieve a desired motion behavior exist. Although there is some effort to derive useful designs by systematic investigations [3]–[9], most are certainly based on trial and error.

The aim of this study is to review and to extend systematic investigations of design aspects in the case of a bending actuator. The actuator should be modular, require little manufacturing effort, and be advantageous for modeling while providing satisfactory bending performance. With these properties, there are two possible applications: 1) customizable actuators that are adaptable to their application with little effort, and 2) research tasks for which single properties of an actuator can easily be changed and for which an accurate model is needed.

The most common techniques for building pneumatic bending actuators are: using materials with different stiffness [10], using a complex morphology (Pneumatic Network) [11], or using parallel chambers [12]. Similar to many others, e.g. [12]–[15], we discuss the latter because of its versatility in motion. The drawback of this solution is the need to manufacture and control multiple chambers instead of only a single one. However, using a single chamber actuator with different material stiffness leads to a predefined relation of stretching and bending, and using a PneuNet additionally involves high manufacturing effort due to the complex geometry.

The study is structured as follows. Information on general design aspects and the final design are presented in section II, followed by the actuator's basic characteristics in section III. Finally, we conclude our findings in section IV.

II. Design

This section is split in two parts. Part A is a general discussion of various design aspects of multi chamber bending actuators. In part B, we rely on these results in order to present our novel design.

A. Design aspects

In the following, we address typical questions a designer might have by reviewing literature on soft robot designs and presenting supplementary investigations. Since universally valid rules for each design aspect are beyond the scope of this study, we demonstrate examples for typical dimensions instead. However, the results are scalable if the proportions remain approximately equal.

We use the bending angle at a given pressure to quantitatively compare different options of the design aspects, knowing that other characteristics, e.g. resistance to external forces, may be of interest as well. Furthermore, we take "soft" aspects, e.g. the manufacturing effort, into account.

1) Number of chambers: Typically, multi chamber bending actuators consist of three chambers [12]–[15], since this is the minimum number required to achieve bending in each spatial direction. Six chambers, with each two equally controlled, provide the same bending capabilities but higher bending moments [13], [16]. However, the optimal number is not necessarily three, as the following examples show.

In [6], important parameters to increase bending are derived from an analytical model, namely the use of the largest pneumatic volume possible. In an example the study presents, the outer dimensions of an actuator are given and the chambers are fitted to the space available. The material volume of walls of three chambers is lower than for a higher number. Conversely, they have the highest pneumatic volume and achieve the largest bending.

In [8], [9], the scenario is a little different since the outer dimensions of the actuator and the cross section of the chambers are given. Here, the pneumatic volume of four chambers is larger than for three chambers and thus bending as well.

To clarify whether a certain number of chambers is beneficial when the ratio of "pneumatic volume/material volume" remains equal, we performed numerical experiments

*Funded by the Deutsche Forschungsgemeinschaft (DFG, German Research Foundation) – 404986830 – SPP2100

[1] The authors are with the Institute for Computational Physics in Engineering, Technische Universität Kaiserslautern, Germany
frederik.lamping@mv.uni-kl.de
kristin.payrebrune@mv.uni-kl.de

2022 IEEE 5th International Conference on Soft Robotics (RoboSoft) | 978-1-6654-0828-8/22/$31.00 ©2022 IEEE | DOI: 10.1109/ROBOSOFT54090.2022.9762087

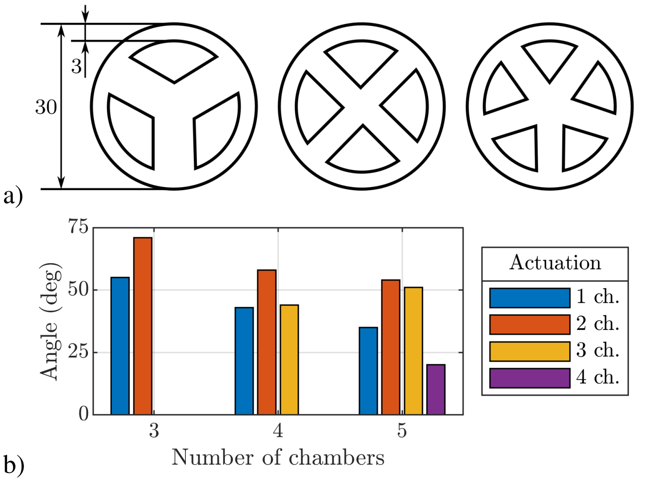

Fig. 1: Actuators with three, four and five chambers a), and respective bending angle for varying number of chambers actuated ($p = 55\,\mathrm{kPa}$) b)

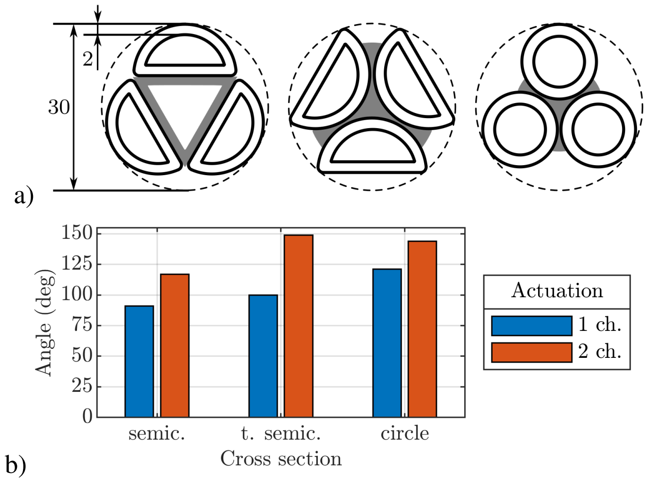

Fig. 2: Actuators with semicircular, turned semicircular, and circular cross sections (rigid linking elements between chambers are indicated gray) a), and respective bending angle for one or two chambers actuated ($p = 55\,\mathrm{kPa}$) b)

with a cylinder containing three, four and five chambers. Similar to the design in [12], the simulated actuator has a cylindrical shape and radial expansion is suppressed by a fiber reinforcement surrounding the whole actuator (not the single chambers). We used Finite Element (FE) simulations in *Abaqus/Standard 2018* with the same element types (material: C3D10H, fiber: B32) and material models (material: hyperelastic, fiber: elastic) as in [10], [17]. From the simulation results, we exported the coordinates of the deformed actuator to *Matlab R2018b* and fitted a circular central axis, from which we determined its bending angle. The actuator is $100\,\mathrm{mm}$ in length, $30\,\mathrm{mm}$ in diameter and consists of Dragon Skin 10 (neo-Hookean, $c_{10} = 42.5\,\mathrm{kPa}$) with Kevlar fibers ($E = 31.067\,\mathrm{MPa}$, $\nu = 0.36$) [17]. As can be seen in Fig. 1a, the chambers keep an outer wall of $3\,\mathrm{mm}$, and the total material and pneumatic volume are independent to their number. In this scenario, three chambers achieve the largest bending, see Fig. 1b.

2) Chamber cross section: The chamber cross section plays an important role for the motion behavior of an actuator. On the one hand, it influences the pneumatic volume and the distance between the center of the module and of the chamber, i.e. the bending moment applied by the chamber [4]. On the other hand, it indirectly influences the amount and arrangement of the surrounding material that opposes bending.

An optimal chamber cross section for an actuator without fiber reinforcement is derived by FE simulations in [3] (elliptic) and [18] (semi-circle). An investigation on single chamber bending actuators with fiber reinforcement identifies a circular cross section as most advantageous: semicircular or rectangular cross sections converge to a circular shape when pressurized, which leads to high stresses at the former edges [19].

We performed supplementary FE simulations on three chamber bending actuators with fiber reinforced chambers and three different cross sections, inspired by the cross sections in [10], see Fig. 2a. The setting of the FE is the same as in *Number of chambers*, the distance between the linking elements indicated in Fig. 2a is $7\,\mathrm{mm}$. Referring to Fig. 2b, the bending angle of the circular cross section is the largest for single chamber actuation. For two chamber actuation, circular and turned semicircular cross sections perform approximately the same. However, in order to prevent high stresses at the edges of the semicircle, a circular cross section should always be preferred.

3) Connection of chambers: The bending mechanism of multi chamber bending actuators requires the chambers to be tied together in order to transform their elongation into bending. Some designs connect the chambers by additional rigid elements [13], [15], while others embed them into a body of silicone [4], [12], [14], [16].

We compared both alternatives by varying the tying mechanism of the actuator with circular chambers that is shown in Fig. 2b: we used linking elements with varying stiffness and distance, and continuous tying by silicone with the same cross section as the linking elements. As long as the distance between linking elements is small enough to prevent buckling, they achieve larger bending angles than a continuous tying by additional silicone that opposes bending. Thus, embedding the chambers into a body of silicone (e.g as in [4], [14]), which means a maximum of additional material, reduces the bending capabilities of an actuator. When the flexible linking elements are stiff enough to keep the chambers in position, there is no difference in bending between rigid and flexible linking elements. A maximum distance between linking elements is hard to define since it depends on the diameter and wall thickness of the chambers and the forces applied to the actuator.

Using linking elements instead of embedding the chambers in silicone has a positive side effect when simulating the actuator with a beam model. This model reduces the structure of the actuator from three dimensions to only one, e.g. by a "geometric superposition" of the behavior of an individual chamber [13], [20], [21]. The simpler the geometry of the chambers is, and the less additional material surrounds them, the more accurate the model is.

4) Reinforcement: A reinforcement controls the radial expansion of an actuator, or its chambers, respectively. The type and position of the reinforcement significantly influence the bending behavior.

There are two possibilities of installing the reinforcement: Either each individual chamber is reinforced, e.g. in [13], or the whole actuator is reinforced at once, e.g. in [14]. The latter increases the maximum bending, since, when only a single chamber is pressurized, it is able to blow up and to increase its cross section. However, this has two important drawbacks: the bending is strongly nonlinear which complicates modeling, and (in the case of friction between the actuator and the reinforcement) the bending depends not only on the pressure level of the chambers, but also on the order in which they are pressurized [4], [8]. Consequently, reinforcing the individual chambers should be preferred.

A bellow structure suppresses radial expansion of a chamber without using a second material, but when the bellows are fully unfolded, it starts to oppose bending due to radial expansion [14]. Another possibility without using a second material is adding a rib structure to the chamber's wall such that the thicker areas prevent radial expansion. However, the stiffness of a rib corresponds to its thickness, while using a rib from a much stiffer material can do the same without necessarily increasing the space required.

The actuators previously used for FE simulations have a fiber reinforcement with counter rotating fibers that prevent torsion, and with a fiber density that suppresses ballooning. This is, independent from the number of chambers, a common technique for many different actuators [10], [12]–[15], [22]. An important drawback of fiber reinforcement is a time-consuming manufacturing process, which can be overcome by using a braided sleeving instead of wrapping fibers around the actuator, e.g. in [13]. However, in a preliminary investigation on individual cylinders, we found that the fiber angle should be as little as possible (perpendicular to the middle axis of the cylinder) [23], while commercially available sleevings typically have larger angles, which, combined with a high fiber density, leads to high friction between reinforcement and chamber. This reduces the stretching capabilities and complicates modeling. An interesting approach to reduce manufacturing effort is the "Instant soft robot" [24]. It is build from a single-use mold that contains a reinforcing structure. After casting and curing, the structure is embedded in silicone and the outer parts of the mold can be removed.

As an additional option, we suggest using rings instead of a fiber or a structure which is cast-in. The rings can be manufactured independently from the chamber with a material of choice (which is stiff enough to prevent radial expansion), and are simply pulled over the chamber. Little

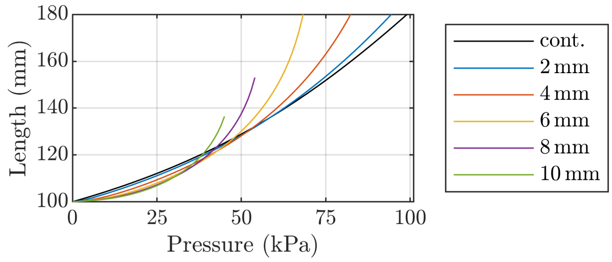

Fig. 3: Stretch of a pneumatic cylinder as a function of pressure for continuous reinforcement and varying distance between ring reinforcement

notches in the chamber wall are sufficient to hold the rings in position. While this method allows fast manufacturing, the chamber balloons between the rings when pressurized, which has a negative impact on pressure resistance, wear, and linearity [7], [19]. However, the intensity of ballooning depends on the inner and outer radius of the chamber, and of the distance between the rings.

In Fig. 3, we demonstrate the influence of the distance between the rings of an individual cylindrical chamber, using the analytic model of a preliminary study [23]. The cylinder is related to the circular cross section in Fig. 4a but with thicker walls. It has an inner radius of $4\,\mathrm{mm}$, an outer radius of $7.5\,\mathrm{mm}$, a length of $100\,\mathrm{mm}$, and also consists of Dragon Skin 10. For the continuous reinforcement, we assume that the outer radius of the cylinder remains constant. As predicted in [7], [19], a larger distance between the rings increases nonlinearity, leading to diverging behavior above a certain pressure level (visible for $8\,\mathrm{mm}$ and $10\,\mathrm{mm}$ in Fig. 3). This effect is well known for balloons made of hyperelastic material [25]. Consequently, a small distance between rings should be preferred, but it does not necessarily need to be chosen as small as any possible. Rather, a reasonable distance depends on the dimensions of the cylinder and the desired stretch. This finding is independent from the material and can be transferred to multi chamber bending actuators.

5) Chamber dimensions: The bending of multi chamber actuators is the result of an interactive pushing and pulling of the chambers that are tied together. As already mentioned in *Connection of chambers*, the simplest configuration of such an actuator in terms of modeling are cylindrical chambers connected by a stiff linking element. With this simplification, the influence of the chamber dimension can be qualitatively derived from the behavior of individual chambers, which has already been studied by many [10], [13], [22], [23], [26].

The axial stretch of a pressurized cylinder with fiber reinforcement, which correlates with the bending of a multi chamber actuator, depends on its material and the ratio of "pneumatic volume/material volume", i.e. the thickness of wall compared to the area of the inner cavity. Interestingly, the additional pressure required to compensate for axial forces depends only on the outer radius of the cylinder and neither on the wall thickness itself nor on the material [23]. Consequently, a suitable design can be found by

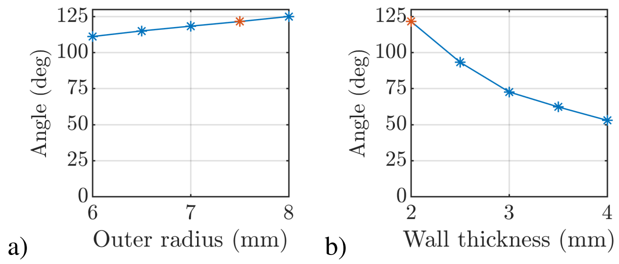

Fig. 4: Bending of an actuator with circular cross section at $p = 55\,\mathrm{kPa}$ for varying outer radius (wall thickness and distance between outer walls of the chambers remain equal) a) and wall thickness (outer radius remains equal) b). The result for the original dimensions of the actuator that is shown in Fig. 2 are indicated orange.

first evaluating the forces an actuator needs to compensate and then choosing the outer radius. As illustrated in Fig. 4a, a change of the outer radius of circular chambers has only little influence on the bending when the distance between the outer walls of the chambers (not between their central points) remains equal. After an outer radius is found, the wall thickness, i.e. the inner radius, determines the stretch and bending behavior of the actuator, see Fig. 4b.

B. *Final design*

From the essentially general discussion in part A, we derived a design approach that requires little manufacturing effort, is modular, and is advantageous for modeling. In brief, the actuator (Fig. 5) consists of three cylindrical chambers, since three chambers promise most efficient bending (*Number of chambers*), and a cylindrical cross section prevents high stresses (*Chamber cross section*). Reinforcing the chambers with rings reduces manufacturing effort (*Reinforcement*) and connecting them with linking elements is both most efficient and advantageous for modeling (*Connection of chambers*). The overall dimensions and that of the chambers are in a range typical for such actuators [10], [13], [14], [26]. The components are constructed in a fashion allowing to adapt individual components independently from the others. In the following, we discuss the components of the actuator and the manufacturing process in detail.

1) Chambers: The outer radius of the chambers is $7.5\,\mathrm{mm}$, the inner radius is $4\,\mathrm{mm}$, as already used in part A (*Reinforcement*). The outer radius is based on the consideration that the base area of an actuator with an overall outer diameter of approximately $30-40\,\mathrm{mm}$ is utilized as best as possible. The inner radius results in a wall thickness of $3.5\,\mathrm{mm}$ allowing relatively fast pouring of the silicone and providing stability to the actuator. However, it can be easily changed by exchanging the central rod of the mold. The outer diameter should not be changed in order to keep adaptability to the other components of the actuator.

In order to find the minimum distance between linking elements, we performed experiments and simulations not shown here. From those we know that the distance without external loads should not be larger than $25\,\mathrm{mm}$. When external forces are expected, a smaller distance should be chosen. We choose the length of the chambers to be $50\,\mathrm{mm}$, since it is a multitude of $25\,\mathrm{mm}$.

The material of the chambers should be pourable and flexible. As typical in soft robotics, we use Dragon Skin 10 and Ecoflex 00-50 (both *Smooth-On Inc., USA*).

2) Reinforcement: The reinforcing rings are pulled over the chamber and are hold in position by little notches in the wall. Since each notch is a weak area, their depth is only $0.3\,\mathrm{mm}$. This is sufficient because the chamber wall presses against the rings when pressurized, forming a self-holding mechanism.

The distance of the rings is a compromise between manufacturing effort and overall flexibility of the actuator against ballooning. Considering Fig. 3, we found that $3.75\,\mathrm{mm}$ is a reasonable distance. Critical ballooning appears when the actuator stretches approximately $75\,\%$.

The rings can be made of any material that is substantially stiffer than the material of the chambers: e.g. ABS (Acrylnitril-Butadien-Styrol-Copolymere), PLA (Polylactic acid), VisiJet M2R (*3D-Systems GmbH, Germany*), or Simpact 85A (Polyurethane, *Smooth-On Inc., USA*). The latter needs to be poured, while the others are printed.

3) End caps: Since the chambers are not embedded into the body of the actuator, they are connected by additional components [13], [15], [27], [28]. The end caps that we propose tie the chambers, provide inlets for the air hoses, and close the inner cavity of the chambers, which accelerates the manufacturing process. They can be made of the same materials as the rings. Since the end caps comprise more material than the rings, a stiff silicone, e.g. ADDV-42 (*R&G Verbundwerkstoffe GmbH, Germany*), can also be used without loosing stability. If more than one “module” is desired, a stacked actuator can be made by using connector caps as presented in Fig. 5c.

Typically, the sealing is the weakness of the chamber and might limit pressurization [6], [29]. We overcome this by a self-holding mechanism. The end caps surround the chambers with a notch for applying glue (Sil-Poxy, *Smooth-On Inc., USA*), see Fig. 5b. By that, the wall of a pressurized chamber pushes against the end caps, which provides additional stability to the sealing. The self-holding mechanism is not necessary if the end caps consist of silicone, because this allows a strong glued connection to the silicone chambers.

4) Linking element: As already mentioned, the chambers should be connected each $25\,\mathrm{mm}$ in order to prevent buckling. Each $50\,\mathrm{mm}$, this is done by an end cap or connector cap. In between, we use linking elements which replace the rings of the reinforcement at the corresponding position, and are also pulled over the chambers. The advantage of linking elements is to reduce the manufacturing effort, and to increase the overall flexibility of the actuator compared to end/connector caps every $25\,\mathrm{mm}$. The linking elements can be made from the same materials as the rings.

5) Possibilities for adaption: The design of the actuator is modular, which is advantageous for customization. Below

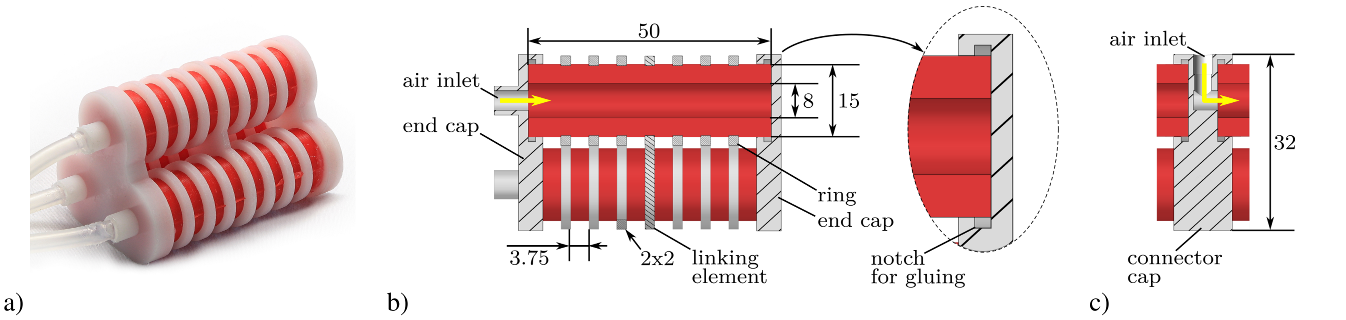

Fig. 5: Modular actuator assembled a), its dimensions and name of its components b), and a connector cap that can be used instead of an end cap to stack modules c). The sideview shows a cut through the middle plane of the actuator.

we present an excerpt of possibilities:

- The *materials* are an important choice in order to define the actuator's characteristics and the manufacturing effort. Using printable materials for the end/connector caps, rings, and the linking element is less time-consuming than pouring.
- The *inner radius* of the chambers has a strong influence on the characteristics of the actuator. It can be changed by exchanging the inner rod of the mold.
- The chambers can be easily cut to a shorter *length* if desired.
- Rings can be easily replaced by *multiple linking elements*, if the actuator has to apply high forces to its surrounding.
- Changing the radial *distance between the chambers* has an impact on the bending moment the actuator is able to apply. This can be done by adapting the end/connector caps, and linking elements.
- Furthermore, a larger distance between chambers leaves room for *additional components*, such as a stiffening element or a universal joint.

Note that the possibilities presented can be implemented by only changing individual components without requiring changes to other components.

6) Manufacturing process: For assembling an actuator, the air hose is glued to the end cap with air inlet, see Fig. 5b. By first pushing the hose through the inlet, such that the tip sticks out the other side, applying some glue, and then pulling it back slightly, a self-holding connection is achieved. Afterwards, the notch of one of the end caps is filled with Sil-Poxy (silicone glue, *Smooth-On Inc., USA*) and the cylinders are inserted to it. In the next step, the rings and linking element are pulled over the chambers. Finally, the notch of the second end cap is filled with glue and the end caps are inserted. Alternatively, a connector cap is used instead of the end cap and the process is repeated.

Due to the modularity of the actuator, components and adaptions of them can be produced in stock, creating a construction kit. In order to reuse the components of a used actuator, or to replace single components, the actuator can be disassembled in the reverse order. When the chambers are removed from the end/connector caps, the cured glue can be cut off with scissors which makes the chambers reusable as well. Due to the strong gluing, it is not possible to remove the chambers from the end/connector caps if the latter consist of silicone.

III. Experimental Characterization

From the multitude of possible configurations, we tested three that are listed in Table I. Types 1 and 2 use stiff components (except the chambers) which reduces potential nonlinear effects. Type 3 is the soft version of type 2.

As can be seen in Fig. 6, we tested single chamber, two chamber, and three chamber actuation. Pressure was increased from 12 kPa in steps of 2 kPa (Ecoflex) and 4 kPa (Dragonskin), respectively, to a level at which ballooning seemed to damage the actuator, using a pneumatic terminal (*Motion Terminal, Festo SE & Co. KG, Germany*). The stretching and bending was determined by image analysis in *Matlab R2018b*, which evaluated the position and the orientation of the end caps.

TABLE I: Configuration of the experimentally tested actuators

Type	Chambers	End caps	Rings/ Linking element
1	Ecoflex 00-50	Visijet M2R	Visijet M2R
2	Dragon Skin 10	Visijet M2R	Visijet M2R
3	Dragon Skin 10	ADDV-42	Simpact 85A

A. Chambers

According to the stiffness of the chamber material, type 1 operates at a lower pressure level than types 2 and 3, see Fig. 6. The maximum possible stretching and bending is independent from the chamber material. Type 3 bends and stretches less due to its flexible rings, see below. For all types, the difference in the maximum bending angle for single chamber actuation and for two chamber actuation is little compared to the simulation in Fig. 2.

For the chamber dimensions chosen, using Ecoflex 00-50 makes an actuator sensitive to manufacturing errors. Due to the softness of the material, one chamber easily deforms differently than the others, which leads to irregular stretch,

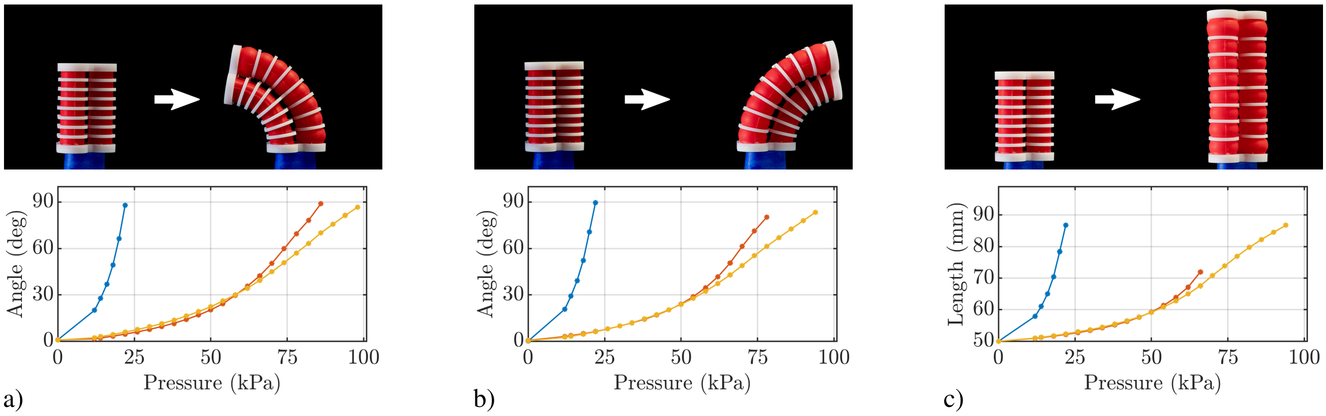

Fig. 6: Single chamber a), two chamber b), and three chamber actuation c) of the tested actuators: type 1 (Ecoflex 00-50/Visijet M2R) in blue, type 2 (Dragon Skin 10/Visijet M2R) in yellow, and type 3 (Dragon Skin 10/ADDV-42/Simpact 85A) in orange. The images show type 2 without pressure and at maximum pressure.

i.e. the actuator slightly bends when the same pressure is applied to all chambers. It took several trials to produce an actuator that stretches purely straight for determining the characteristics shown in Fig. 6. Consequently, the wall thickness should be increased when using Ecoflex 00-50.

However, similar to the "Instant soft robot" presented in [24], the characteristics of our actuator with chambers made of Dragon Skin 10 are comparable to a "STIFF-FLOP" made of Ecoflex 00-50 [4], [14]. On the one hand, this is because the relation of pneumatic to material volume is different [24]. On the other hand, there is no friction between reinforcement and chamber wall when using separated reinforcing elements.

B. Evaluation of the reinforcement

We chose a ring reinforcement in order to reduce manufacturing effort, accepting that ballooning will occur. Due to ballooning, the maximum stretching and bending of our actuator is lower than that of the "STIFF-FLOP" [4], [14], as shown in Table II. The "Instant soft robot" [24] shares this issue because it also consists of separated reinforcing elements instead of a fiber or a braided sleeving. Since the distance between the reinforcing elements is smaller than in our case, ballooning appears at higher stretch. If needed, the distance between rings of our actuator could be reduced as well.

Another difficulty arises when flexible rings made of Simpact 85A are used. Since the notches that hold the rings in position are flat, flexible rings tend to roll out of them when ballooning occurs. We reduced this effect by using only linking elements not rings to reinforce type 3, see Fig. 7. Another possibility is to increase the number of rings or linking elements, respectively. However, using a flexible reinforcement is still critical and further development should be made to prevent rolling, as can be seen from the results in Fig. 6. Type 2 and 3 bend and stretch equally up to 58 kPa, whereas they diverge at higher pressure due to ballooning of type 3. For three chamber actuation, ballooning occurred at lower pressure than for other actuation.

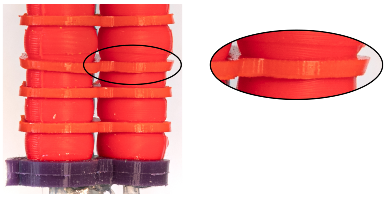

Fig. 7: Deformed reinforcement of type 3 at 66 kPa (three chamber actuation)

Comparing the three configurations of our actuator tested, type 2 was the easiest to handle. Its chamber material Dragon Skin 10 suppresses the effect of manufacturing errors and its stiff rings do not tend to roll for higher pressure.

IV. Conclusions

In this study, we discuss design aspects of building a multi chamber bending actuator, reviewing literature and presenting supplementary investigations. The discussion of the general design aspects of multi chamber bending actuators in section IIA raises some aspects that are a compromise between conflicting interests, e.g. linearity and stability versus manufacturing effort in reinforcement. Consequently, it is not possible to find a generally optimized design.

The actuator we propose focuses on being advantageous for manufacturing and modeling. To achieve the former, we use modular components that can be produced in stock. In contrast to other bending actuators, the reinforcement consists of rings which are pulled over the chamber. Due to modularity, adapted versions of the actuator can be build with little effort. Using cylindrical chambers connected by linking elements is geometrically simple and therefore advantageous for modeling, since beam models are often based on a superposition of the behavior of an individual chamber [13], [20].

Experimental investigation shows that our actuator has a clearly lower performance than the "STIFF-FLOP" [4], [14], but only a slightly lower performance than the "Instant soft robot" [24]. Especially the ring reinforcement, which was

TABLE II: An overview of the maximum bending angle or stretch, respectively, of comparable actuators. Type 2 is chosen for comparison due to its stability at high pressure.

Study	Name	Length/Diam.	Material	p_{max}	1 chamb.	2 chamb.	3 chamb.
Cianchetti et al. [14]	STIFF-FLOP	$50/35\,\mathrm{mm}$	Ecoflex 00-50	$65\,\mathrm{kPa}$	$120\,\mathrm{deg}$	$80\,\mathrm{deg}$	$86\,\%$
Fraś et al. [4]	STIFF-FLOP	$50/35\,\mathrm{mm}$	Ecoflex 00-50	$150\,\mathrm{kPa}$	$110\,\mathrm{deg}$	$140\,\mathrm{deg}$	-
Fraś et al. [24]	Instant soft robot	$38/22\,\mathrm{mm}$	Dragon Skin	$180\,\mathrm{kPa}$	$91\,\mathrm{deg}$	$97\,\mathrm{deg}$	$90\,\%$
This study	Type 2	$50/42\,\mathrm{mm}$	Dragon Skin	$94\,\mathrm{kPa}$	$87\,\mathrm{deg}$	$83\,\mathrm{deg}$	$74\,\%$

chosen in order to reduce the manufacturing effort, limits maximum stretching and bending. Taking this disadvantage into account, our actuator contributes to building and modeling customizable soft robotic systems with little effort. Future work will focus on improving the ring reinforcement. Probably, our design could be matched with that of the "Instant soft robot" [24], which would reduce ballooning while keeping simplicity of manufacturing and modeling.

REFERENCES

[1] C.-Y. Chu and R. M. Patterson, "Soft robotic devices for hand rehabilitation and assistance: a narrative review," *Journal of NeuroEngineering and Rehabilitation*, vol. 15, no. 1, feb 2018.

[2] P. Boyraz, G. Runge, and A. Raatz, "An overview of novel actuators for soft robotics," *Actuators*, vol. 7, no. 3, 2018. [Online]. Available: http://www.mdpi.com/2076-0825/7/3/48

[3] K. Suzumori, T. Maeda, H. Wantabe, and T. Hisada, "Fiberless flexible microactuator designed by finite-element method," *Mechatronics, IEEE/ASME Transactions on*, vol. 2, no. 4, pp. 281–286, 1997.

[4] J. Fras, J. Czarnowski, M. Macias, J. Glowka, M. Cianchetti, and A. Menciassi, "New STIFF-FLOP module construction idea for improved actuation and sensing," in *2015 IEEE International Conference on Robotics and Automation (ICRA)*. IEEE, may 2015.

[5] H. Zhang, M. Y. Wang, F. Chen, Y. Wang, A. S. Kumar, and J. Y. H. Fuh, "Design and development of a soft gripper with topology optimization," in *2017 IEEE/RSJ International Conference on Intelligent Robots and Systems (IROS)*. IEEE, sep 2017.

[6] A. Garriga-Casanovas, I. Collison, and F. R. y Baena, "Toward a common framework for the design of soft robotic manipulators with fluidic actuation," *Soft Robotics*, vol. 5, no. 5, pp. 622–649, oct 2018.

[7] J. Fras and K. Althoefer, "Soft fiber-reinforced pneumatic actuator design and fabrication: Towards robust, soft robotic systems," in *Towards Autonomous Robotic Systems*. Springer International Publishing, 2019, pp. 103–114.

[8] J. A. Lenssen, H. Naghibi, and M. Abayazid, "Evaluation of design aspects of modular pneumatic soft robotic endoscopes," in *2019 2nd IEEE International Conference on Soft Robotics (RoboSoft)*. IEEE, apr 2019.

[9] H. Naghibi, M. W. Gifari, W. Hoitzing, J. W. Lageveen, D. van As, S. Stramigioli, and M. Abayazid, "Development of a multi-level stiffness soft robotic module with force haptic feedback for endoscopic applications," in *2019 International Conference on Robotics and Automation (ICRA)*. IEEE, may 2019.

[10] P. Polygerinos, Z. Wang, J. T. B. Overvelde, K. C. Galloway, R. J. Wood, K. Bertoldi, and C. J. Walsh, "Modeling of soft fiber-reinforced bending actuators," *IEEE Transactions on Robotics*, vol. 31, no. 3, pp. 778–789, 2015.

[11] B. Mosadegh, P. Polygerinos, C. Keplinger, S. Wennstedt, R. F. Shepherd, U. Gupta, J. Shim, K. Bertoldi, C. J. Walsh, and G. M. Whitesides, "Pneumatic networks for soft robotics that actuate rapidly," *Advanced Functional Materials*, vol. 24, no. 15, pp. 2163–2170, 2014.

[12] K. Suzumori, S. Iikura, and H. Tanaka, "Development of Flexible Microactuator and its Applications to Robotic Mechanisms," in *1991 IEEE International Conference on Robotics and Automation (ICRA)*, 1991, pp. 1622–1627.

[13] D. Trivedi, A. Lotfi, and C. D. Rahn, "Geometrically exact dynamic models for soft robotic manipulators," in *2007 IEEE/RSJ International Conference on Intelligent Robots and Systems (IROS)*, 2007, pp. 1497–1502.

[14] M. Cianchetti, T. Ranzani, G. Gerboni, I. De Falco, C. Laschi, and A. Menciassi, "Stiff-flop surgical manipulator: Mechanical design and experimental characterization of the single module," in *2013 IEEE/RSJ International Conference on Intelligent Robots and Systems (IROS)*, 2013, pp. 3576–3581.

[15] L. Lindenroth, A. Soor, J. Hutchinson, A. Shafi, J. Back, K. Rhode, and H. Liu, "Design of a soft, parallel end-effector applied to robot-guided ultrasound interventions," in *2017 IEEE/RSJ International Conference on Intelligent Robots and Systems (IROS)*. IEEE, sep 2017.

[16] H. Abidi, G. Gerboni, M. Brancadoro, J. Fras, A. Diodato, M. Cianchetti, H. Wurdemann, K. Althoefer, and A. Menciassi, "Highly dexterous 2-module soft robot for intra-organ navigation in minimally invasive surgery," *The International Journal of Medical Robotics and Computer Assisted Surgery*, vol. 14, no. 1, p. e1875, dec 2017.

[17] P. Polygerinos, K. Galloway, Z. Wang, F. Connolly, J. T. B. Overvelde, and H. Young. Finite element modeling. Accessed on: 10-18-2021. [Online]. Available: https://softroboticstoolkit.com/book/fr-modeling

[18] Y. Elsayed, A. Vincensi, C. Lekakou, T. Geng, C. Saaj, T. Ranzani, M. Cianchetti, and A. Menciassi, "Finite element analysis and design optimization of a pneumatically actuating silicone module for robotic surgery applications," *Soft Robotics*, vol. 1, no. 4, pp. 255–262, 2014.

[19] J. Fraś, "Depth-map-based shape recognition of soft continuum manipulator body," in *Automation 2017*. Springer International Publishing, 2017, pp. 300–307.

[20] S. M. Mustaza, Y. Elsayed, C. Lekakou, C. Saaj, and J. Fras, "Dynamic modeling of fiber-reinforced soft manipulator: A visco-hyperelastic material-based continuum mechanics approach," *Soft Robotics*, vol. 6, no. 3, pp. 305–317, jun 2019.

[21] G. Bao, L. Chen, Y. Zhang, S. Cai, F. Xu, Q. Yang, and L. Zhang, "Trunk-like soft actuator: Design, modeling, and experiments," *Robotica*, vol. 38, no. 4, pp. 732–746, jul 2019.

[22] J. Bishop-Moser, G. Krishnan, C. Kim, and S. Kota, "Design of soft robotic actuators using fluid-filled fiber-reinforced elastomeric enclosures in parallel combinations," in *2012 IEEE/RSJ International Conference on Intelligent Robots and Systems (IROS)*, oct 2012, pp. 4264–4269.

[23] F. Lamping and K. M. de Payrebrune, "A virtual work model for the design and parameter identification of cylindrical pressure-driven soft actuators," pp. 1–16, oct 2021.

[24] J. Fras, J. Glowka, and K. Althoefer, "Instant soft robot: A simple recipe for quick and easy manufacturing," in *2020 3rd IEEE International Conference on Soft Robotics (RoboSoft)*. IEEE, may 2020.

[25] A. Needleman, "Inflation of spherical rubber balloons," *International Journal of Solids and Structures*, vol. 13, no. 5, pp. 409–421, 1977.

[26] A. Sedal, D. Bruder, J. Bishop-Moser, R. Vasudevan, and S. Kota, "A continuum model for fiber-reinforced soft robot actuators," *ASME J. Mech. Robot.*, vol. 10, no. 2, p. 024501, 2018.

[27] R. Kang, D. Branson, T. Zheng, E. Guglielmino, and D. Caldwell, "Design, modeling and control of a pneumatically actuated manipulator inspired by biological continuum structures," *Bioinspiration & Biomimetics*, vol. 8, no. 3, p. 036008, 2013. [Online]. Available: http://stacks.iop.org/1748-3190/8/i=3/a=036008

[28] X. Peng, N. Zhang, L. Ge, and G. Gu, "Dimension optimization of pneumatically actuated soft continuum manipulators," in *2019 2nd IEEE International Conference on Soft Robotics (RoboSoft)*. IEEE, apr 2019.

[29] F. Schmitt, O. Piccin, L. Barbé, and B. Bayle, "Soft robots manufacturing: A review," *Frontiers in Robotics and AI*, vol. 5, jul 2018.